Applied Thermal Engineering 114 (2017) 756–769

Contents lists available at ScienceDirect

Applied Thermal Engineering

journal homepage: www.elsevier.com/locate/apthermeng

Research Paper

Optimal economic dispatch of FC-CHP based heat and power micro-grids

Morteza Nazari-Heris *, Saeed Abapour, Behnam Mohammadi-Ivatloo

Smart Energy Systems Laboratory, Faculty of Electrical and Computer Engineering, University of Tabriz, Tabriz, Iran

HIGHLIGHTS

- The multi objective economic/environmental heat and power MG dispatch is solved.
- The heat and power MG include FC, CHP, boiler, storage system, and heat buffer tank.
- Multi objective scheduling of heat and power MG is solved using ε-constraint method.
- DR program is employed in the stochastic programming of heat and power MG dispatch.
- The uncertainties for load demand and price signals are taken into account.

ARTICLE INFO

Article history:
Received 25 July 2016
Revised 28 November 2016
Accepted 6 December 2016
Available online 8 December 2016

Keywords:
Fuel cell
Combined heat and power (CHP)
Economic dispatch
Demand response (DR) program
Heat and power micro-grid (MG)
Storage devices
ε-Constraint method

ABSTRACT

Micro-grids (MGs) are introduced as a solution for distributed energy resource (DER) units and energy storage systems (ESSs) to participate in providing the required electricity demand of controllable and non-controllable loads. In this paper, the authors study the short-term scheduling of grid-connected industrial heat and power MG which contains a fuel cell (FC) unit, combined heat and power (CHP) generation units, power-only unit, boiler, battery storage system, and heat buffer tank. The paper is aimed to solve the multi-objective MG dispatch problem containing cost and emission minimization with the considerations of demand response program and uncertainties. A probabilistic framework based on a scenario method, which is considered for load demand and price signals, is employed to overcome the uncertainties in the optimal energy management of the MG. In order to reduce operational cost, time-of-use rates of demand response programs have been modeled, and the effects of such programs on the load profile have been discussed. To solve the multi-objective optimization problem, the ε-constraint method is used and a fuzzy satisfying approach has been employed to select the best compromise solution. Three cases are studied in this research to confirm the performance of the proposed method: islanded mode, grid-connected mode, and the impact of time of the use-demand response program on MG scheduling.

1. Introduction

Micro-grids (MGs) are defined as the integration of distributed energy resource (DER) units, energy storage systems (ESSs), and a group of controllable and non-controllable loads. MGs can be used in different modes including connected to a grid or islanded modes. MG plays a key role in the moderation of power balance of supply and demand by connecting to a grid, which sells power to the grid or buys power from the grid. In the separated mode, MG is apart from the grid, in which the customers purchase a reliable power from MG, taking into consideration the DG bids [1,2]. Considering a MG integrated with DER, combined heat and power (CHP) systems, and energy storage technologies, significant advantages such as an environmental friendly energy, low-cost electricity, and reliable energy could be attained. CHP systems play an important role in reducing the cost of thermal energy generation by recovering the heat wasted during the generation of electrical energy [3]. CHP economic dispatch (CHPED) aims to minimize the cost of heat and power generation in which the mutual dependency of heat and power and the heat-power capacity of cogeneration units should be taken into account [4]. The operation of CHP systems is optimized in [5] with the consideration of cost-saving uncertainties associated with the operation of CHP system. The optimal solution for the CHPED optimization problem is obtained in [6,7], considering heat-power dependency characteristics. A research study on a micro-CHP system is provided in [8] which developed a Gamma-type Stirling engine for biomass energy to

* Corresponding author.
E-mail addresses: mnazari94@ms.tabrizu.ac.ir (M. Nazari-Heris), sa.abapour@gmail.com (S. Abapour), mohammadi@ieee.org (B. Mohammadi-Ivatloo).

http://dx.doi.org/10.1016/j.applthermaleng.2016.12.016
1359-4311/

Nomenclature

π_l	probability of the lth load demand scenario
π_ρ	probability of the pth price scenario
π_s	probability of the sth scenario
$P^D_{h,s}$	the initial electric load demand at hth load level in scenario s (MWh)
$P^{DR}_{h,s}$	the electric load demand after applying DR program at hth load level in scenario s
$ldr_{h,s}$	the amount of shifted load from other load level to hth load level in scenario s
$DR_{h,s}$	the participation factor of load in DR program at hth load level in scenario s
$DR^{\max}_h$	maximum participation factor in DR program
$P^{\max FC}$	total power produced at interval h by FC unit
P^{FC-th}_h	the potential thermal power of FC
$P^{FC-H_2}_h$	equivalent electric power for hydrogen production (kW)
P^{FC}_h	electrical power produced by FC unit at interval h
P_a	power for auxiliary devices (kW)
η_h	fuel cell efficiency at interval h
r_{th}	the thermal to electrical energy ratio
H_2	the amount of the generated hydrogen
f	conversion factor (kg of hydrogen/kW of electric power)
v_{cell}	cell operating voltage
HT_h	the stored hydrogen amount at interval h
η^{st}	hydrogen storage efficiency
$P^{FC-H_2}_{h,usage}$	the secondary hydrogen stream amount at interval h (kW)
UH^s_h, UH^{disc}_h	binary variable for charge and discharge of hydrogen
$P^{FC-H_2}_{s,\max}, P^{FC-H_2}_{disc,\max}$	equivalent maximum charge and discharge electric power for hydrogen production (kW)
PLR_h	electrical generated power/maximum power
C_{ng}	price of natural gas for FC ($/kWh)
C_{pump}	hydrogen pumping cost ($/kWh)
OM	the operation and maintenance cost of the FC ($/kWh)
C_{FC}	cost function of FC unit
$P^{FC-\min}, P^{FC-\max}$	maximum and minimum limits of FC power
$P^{CHP}_{i,h}$	generated power from CHP unit i at time h (MW)
$H^{CHP}_{i,h}$	generated heat from CHP unit i at time h (MWth)
A, B, C, D	four marginal points of the FOR in each two types of CHP units
E, F	two marginal points of the FOR in second type of CHP unit
$V^{CHP}_{i,h}$	binary variable for commitment status of the CHP unit i at time h
M	a sufficient large number
$X_{1,h}/X_{2,h}$	operation state of the CHP units in the first/second convex section of FOR
$C(P^{CHP}_h, H^{CHP}_h)$	cost function of CHP unit at time h
$a_i, b_i, c_i, d_i, e_i, f_i$	cost function coefficients of CHP units
P^{PO}_h	generated power from power-only unit at time h (MW)
$P^{PO-\min}, P^{PO-\max}$	minimum and maximum power limits of power-only unit
H^b_h	Generated heat from boiler unit at time h (MWth)
$H^{b-\min}, H^{b-\max}$	minimum and maximum heat limits of boiler unit
$C(P^{PO}_h)$	cost function of power-only unit at time h
λ_{po}	the price of power of a power-only unit in hours hth ($/MW h)
$C(H^b_h)$	cost function of boiler unit at time h
λ_b	the price of power of boiler unit in hours hth ($/MWth h)
SU^i_h, SD^i_h	binary variable of start-up/shut-down status for the units at time h
$P^c_{h,s}, P^{disc}_{h,s}$	charging/discharging power of battery (kW)
$P^{c,\max}_h, P^{disc,\max}_h$	maximum charging/discharging power (kW)
$b^c_{h,s}, b^{disc}_{h,s}$	binary variable of charging/ discharging states
$ES_{h,s}$	capacity of battery (kWh)
$ES^{\min}_k, ES^{\max}_k$	minimum/maximum energy stored in battery (kWh)
η^C, η^{disc}	charging/discharging efficiency of battery k
$\overline{H}_h$	total produced heat (MWth)
H_h	real heat production (including loss or extra generation) (MWth)
$\beta_{loss}, \beta_{gain}$	heat generation loss/excess for the CHP unit during startup/shutdown period
B_h	available heat in the heat buffer tank at time h (MWth)
H^{load}_h	heat demand at time h (MWth)
η	heat loss rate for the heat buffer tank
$B_{\min}, B_{\max}$	minimum/maximum heat buffer tank capacity (MWth)
$B^{charge}_{\max}, B^{discharge}_{\max}$	the maximum charge (discharge) rate of the storage (MWth)
$\lambda_{h,s}$	the price of power at time h ($/MW h)
$P^{G,sell}_{h,s}, P^{G,buy}_{h,s}$	the amount of electricity sold/procured to the network at time h and scenario s (MW h)
$C_{j,SU}, C_{j,SD}$	startup/shutdown cost of generation facility ($)
$C^{\deg}_k$	cost for battery degradation ($/kWh)
$E^{CHP}_h, E^{FC}_h, E^{PO}_h, E^G_h$	emission values of each units in MG (ton/day)

be used in the micro-CHP system for generating power and heat by biomass fuels.

Distributed generation (DG) and distributed storage (DS) are defined as two major references of DERs. Ref. [9] investigates optimal set points of DERs and storage devices by utilizing an expert energy management system which aims to minimize the total operation cost as well as emission. In this reference, the wind speed is furcated using an artificial neural network (ANN), and the possible availability of power generation of wind turbines is attained. ANN modeling is employed in [10–12] which ensures the importance of this method in solving prediction problems. In [10], the power of the solar Stirling heat engine is estimated by employing a hybrid genetic algorithm and particle swarm optimization-based neural network (HGAPSO-ANN). The method proposed in this reference integrates the local search ability of GA and PSO methods. The authors have introduced a least square support vector machine (LSSVM) in [11] to predict the output power and shaft torque of Stirling engines. A parametric and GMDH-type neural network is employed in [12] for to study a 25-W fabricated PEM fuel cell. A value-based model for analyzing DGs, including fuel cells, mini-gas turbines, and solar PV in terms of optimal types, sizes, and locations is proposed in [13] in which GA is utilized. A dynamic modeling and control strategy for a sustainable MG which is supplied by PV and WT have been introduced in [14] in which the rapid solar irradiance alteration and alteration of wind energy have been taken into consideration.

Considering the significant enhancement of demand and limited generation capacities, demand response (DR) programs are introduced as an effective solution for handling load increment. The U.S. department of energy (DOE) has introduced DR programs as the ability of industrial, residential, and commercial customers to alter energy consumption patterns following the alteration of the price of electricity during a time period or paying incentives for considering reasonable prices and attaining power system reliability. DR programs play a key role in the optimal scheduling of MGs, which should be taken into account especially when renewable sources exist [15]. Power trading and management between MGs with DR and DS (DRaDS) are facilitated by introducing an agent-based energy management system in [16]. This reference aims to decrease the peak demand and minimize the cost of electricity using diversity in load consumption patterns of the customers and energy availability from the DER, DS, and DR. In [17], a two-level architecture is presented to manage the distributed energy resource for multiple MGs which utilizes a multi-agent system (Mas) for modeling market scenario with an electricity purchaser and an electricity seller. A novel optimal scheduling of a CHP-based MG which considers DR programs, ESS, and three types of thermal plants, is presented in [18]. In this reference, DR is modeled as virtual generation units, and the minimization of total operation cost and of CHP-MG in an OPF-formulation and the minimization of the DGs' emission are handled in a multi-objective self-scheduling problem. An employment of an agent demand-side management framework is introduced in [19] which forms a virtual market environment for neighboring MGs to trade with one another. A similar agent-based energy management system is presented in [20] in which a new incentive mechanism known as priority banking is introduced.

In [21], an adaptive modified firefly algorithm (AMFA) is implemented to obtain the optimal solution of a MG operation. The grid-connected MG investigated in this reference consists of WT, PV, micro-turbine, fuel cell, and energy storage devices. To minimize the operation cost of fuel cell power plant, the particle swarm optimization algorithm is employed in [22] in which various tariffs are taken into account for electrical energy purchase and sell in each hour of the day. [23] provides the optimal solution of a PEM fuel cell power plant (FCPP) which is connected to a small-scale MG, utilizing the evolutionary programming (EP) optimization procedure. The capability of purchasing and selling electricity from the local grid, and considering thermal output from the fuel cell and the required thermal energy from the grid are remarked in this reference.

One of the most important renewable energy sources taken into account in numerous studies in recent years is the fuel cell power plant. Fuel cell has considerable advantages including high efficiency, high level of availability, simple structure and operation, high reliability, and the capability of following load alterations. Proton Exchange Membrane (PEM) is a type of fuel cell power plant in which the unused capacity of the plant can be used as a hydrogen-production source [24]. The generated hydrogen can be utilized in two different modes, including (a) stored in a hydrogen tank to supply electricity in the high power demand situation, or (b) sold to other costumers [25]. In hydrogen storage systems, hydrogen is generated with an electrolyzer when the power demand of the grid is less than the power delivered by RES. The stored hydrogen can be utilized for electricity generation by means of a fuel cell in peak demand intervals [26]. The low working temperature of PEM fuel cells power plants, which is between 80 °C to 100 °C, and their fast startup are the significant advantages of these types of fuel cell power plants which are best suited for residential and vehicular applications [27].

Multi-objective optimization problems are defined as problems including more than one objective function to be solved, simultaneously. Various branches of science including engineering, economics, and logistics can employ multi-objective optimization problems. In [28], an irreversible Carnot refrigerator is studied with two optimization scenarios. The first scenario is specified to maximize the ecological coefficient of performance (ECOP), exergy input to the system, and cooling load. The second scenario maximizes the ECOP, exergy input to the system, and ECP. Each scenario is solved using multi-objective optimization algorithms. The multi-objective optimization of the solar-powered Stirling engine is analyzed in [29] which aims to maximize thermal efficiency, entrance loss rate and power output, and minimize the rate of entropy generation in the engine. In this reference, a non-dominated sorting genetic algorithm (NSGA-II) is used to solve the problem. Three conflicting objectives are considered for solving the multi-objective optimization for Stirling engine systems in [30]. The objectives in this reference include maximizing output power and thermal efficiency and minimizing the rate of entropy generation. The authors have implemented the multi-objective optimization based on an evolutionary approach in [31] which studied heating load, thermo-economic benchmark, and the coefficient of performance (COP) of the system. In [32], NSGA is applied to optimize dimensionless power density and thermal efficiency of the Braysson cycle. An integration of NSGA-II and multi-objective evolutionary method is utilized to define the optimal solution of the problem. The multi-objective optimization is studied in [33] for analyzing the performance of irreversible four-temperature-level refrigeration which employed an evolutionary algorithm to prepare the optimal solution.

The principal contribution of this paper is attaining the optimal scheduling of a grid-connected industrial MG, taking into account CHP generation units, fuel cell, one power-only unit, boiler, and storage devices, and considering the DR program. The fuel cell generation unit has the capability of supplying electrical and thermal energy and hydrogen. The exact electrical and heat modeling of the fuel cell unit along with two types of CHP units have not been presented in previous papers. Moreover, the CHP generation unit, one power-only unit, and boiler are considered to produce part of electrical and heat demand. The MG is supposed to encompass storage devices including battery storage system and heat buffer tank which are implemented for storing electrical and heat demand, respectively. Two competing objective functions are taken into account as the minimization of total operation cost and reduction of emission from energy consumption of MG. In order to reduce operational cost, time-of-use rates of DR programs are modeled and their influence on load profile is analyzed. A probabilistic framework which is based on a scenario method is introduced to solve the MG scheduling problem, considering the uncertainties of load demand and price signals. The ε-constraint method is utilized for to solve the multi-objective optimization problem in this paper, which implemented a fuzzy satisfying approach for selecting the best compromise solution. This study has implemented the proposed method on three cases to ensure the performance of the method. The contributions of this paper can be summarized as follows:

- The multi-objective economic/environmental heat and power MG dispatch is solved in this research study using the ε-constraint method.
- The heat and power MG includes a fuel cell unit, combined heat and power (CHP) units, power-only unit, boiler, storage system, and heat buffer tank.
- The fuel cell unit studied in this paper is capable of producing power and heat in addition to storing hydrogen to be utilized in peak demand hours.
- A demand response program is employed in the stochastic programming of heat and power MG dispatch, and the effects of the program and its results are analyzed.
- The uncertainties for load demand and price signals are taken into account in the solution of MG economic dispatch.

The paper is organized as follows: Problem formulation is presented in Section 2. Section 3 proposes the solution method. Simulation results are provided in Section 4. Finally, the paper is concluded in Section 5.

2. Problem formulation

In this paper, the uncertainty of load demand and market price is modeled by a scenario-based approach. Uncertainty scenarios of the market price and load demand are autonomous, so that the total number of scenarios can be calculated by multiplying the scenarios of each element as follows [34]:

$$\pi_s = \pi_l \times \pi_p \tag{1}$$

The total number of scenarios indicated by N_S will be $l \times p$ states. Nine scenarios are considered in this study. Load demand uncertainty states are 0.94, 1, and 1.06. Moreover, the uncertainty states of power market price are 0.94, 1, and 1.08.

2.1. Electric load with demand response

In this paper, it is assumed that load can be shifted from a high market price time interval to low price time interval; in accordance TOU-DR programs are applied. The electrical load based on the DR program could be defined as follows:

$$P^{DR}_{h,s} = P^{D}_{h,s} + ldr_{h,s} \tag{2}$$

$$ldr_{h,s} = DR_{h,s} \times P^{D}_{h,s} \tag{3}$$

$$\sum_{h=1}^{24} ldr_{h,s} = 0 \tag{4}$$

$$DR^{\min}_{h} < DR_{h,s} < DR^{\max}_{h} \tag{5}$$

Eq. (2) expresses load demand after DR implementation in the same period. The moveable demand has a variable size in each period, which is defined by $DR_{h,s}$ and represented by (3). Eq. (4) states that the total amount of shifted load over a daily period will be equal to zero. A constraint (5) limits the maximum amount of $DR_{h,s}$ in each period by $DR^{\max}_{h}$, which is considered to be 30% here. $DR^{\min}_{h}$ is also −30% here.

2.2. Economic model of fuel cell

This study considers the local fuel cell (FC) for MGs to supply part of the demand load. For this purpose, it is assumed that the FC unit provides electrical energy, recovered thermal energy, and hydrogen production to storage.

It has been assumed in a number of recent studies that the FC unit generates thermal energy almost equal to the electrical energy in full load conditions [23].

The following equation shows that the recovered thermal power from the FC depends on electric and hydrogen output:

$$H^{FC}_{h} = r_{th}\left(P^{FC-H_2}_{h} + P^{FC}_{h} + P_a\right) \tag{6}$$

In the full load condition, thermal efficiency which is defined by r_{th} is considered equal to one [23]. P^{FC-th}_{h} can be stored in a heat buffer tank for future use.

2.2.1. Generated hydrogen of FC unit

When power generation is more than load demand, the extra capacity of the FC unit produces hydrogen, and the generated hydrogen is stored to be used in peak load time intervals.

In Eq. (7), $P^{FC-H_2}_{h}$ is an equivalent electrical power factor to express the generated hydrogen value. The equivalent hydrogen in Eq. (7) is expressed in (kg/s), and its amount is calculated as follows [24]:

$$H_2 = f\,\frac{P^{FC-H_2}_{h}}{v_{cell}} \tag{7}$$

where v_{cell} is 0.6 V. The generated hydrogen is given in Eq. (8).

$$P^{FC-H_2}_{h} = P^{\max\ FC} - P^{FC}_{h} - P_a \tag{8}$$

According to Fig. 1, the hydrogen generated by the FC unit is stored in a hydrogen tank and is converted to electric energy during peak load time to supply load demand in MG. This strategy reduces the MG operational costs and increases the system's overall efficiency [35].

The equivalent electric storage of hydrogen in the tank is stated as the following equations:

$$HT_h = HT_{h-1} + \eta^{st} \times P^{FC-H_2}_{h} - P^{FC-H_2}_{h,usage} \tag{9}$$

$$HT^{\min} \leqslant HT_h \leqslant HT^{\max} \tag{10}$$

$$0 \leqslant P^{FC-H_2}_{h} \leqslant UH^{s}_{h} \cdot P^{FC-H_2}_{s,\max}, \quad 0 \leqslant P^{FC-H_2}_{h,usage} \leqslant UH^{disc}_{h} \cdot P^{FC-H_2}_{disc,\max} \tag{11}$$

$$UH^{s}_{h} + UH^{disc}_{h} \leqslant 1; \quad UH^{s}_{h}, UH^{disc}_{h} \in \{1, 0\} \tag{12}$$

The stored hydrogen amount, HT_h at hth hour can be calculated by Eq. (9). The constraint (10) indicates the level of hydrogen stored in a tank. Charge and discharge rates of hydrogen are expressed by (11). In constraint (12), it is assumed that hydrogen at each time can only be charged or discharged.

In a number of studies, FC efficiency has been assumed about 36%, while its value can vary according to the generated electrical energy [24]. In this paper, the ratio of generated electric power to maximum power is expressed as part load ratio (PLR) and is shown in Fig. 2. The mathematical formulation for this curve and the thermal efficiency can be approximated as follows:

$$\begin{aligned}&\text{For } PLR_h < 0.05\\ &\eta_h = 0.272, \quad r_{th} = 0.68\end{aligned} \tag{13}$$

$$\begin{aligned}&\text{For } PLR_h \geqslant 0.05\\ &\eta_h = 0.9033 \times PLR^5_h - 2.996 \times PLR^4_h + 3.6503 \times PLR^3_h - 2.0704\\ &\quad \times PLR^2_h + 0.4623 \times PLR_h + 0.3747\end{aligned} \tag{14}$$

$$\begin{aligned}r_{th,h} = {}& 1.078 \times PLR^4_h - 1.974 \times PLR^3_h + 1.500 \times PLR^2_h - 0.282\\ & \times PLR_h + 0.6838\end{aligned} \tag{15}$$

The cost function of FC is considered as follows:

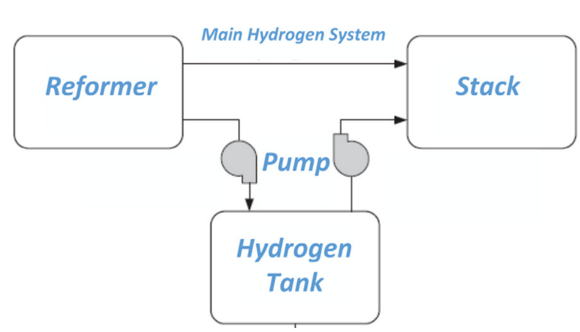

Fig. 1. Hydrogen streams.

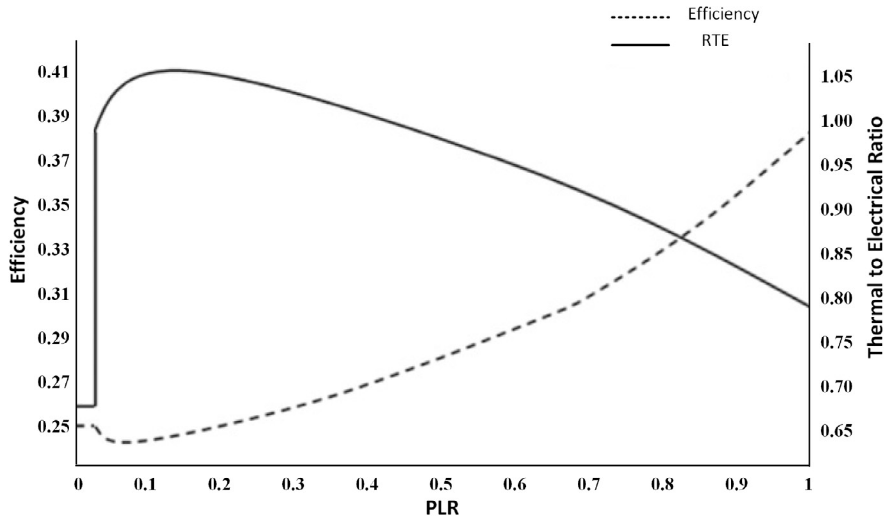

Fig. 2. Performance curve of the FC unit.

$$C_{FC} = \sum_{h=1}^{T} \left[\left(\frac{P_h^{FC} + P_h^{FC-H_2} + P_a}{\eta_h} \times C_{ng} \right) + \eta^{st} \times P_h^{FC-H_2} \times C_{pump} + P^{FC-\max} \times OM \right] \times \tau_h \tag{16}$$

In Eq. (16), the daily fuel cost of the FC unit ($) is expressed by the first term. The daily hydrogen storage cost ($) is presented by the second term. The third term is the operational and maintenance cost of the FC unit ($).

The operation limits of FC unit can be expressed as follows:

$$P^{FC-\min} \times V_h^{FC} < P_h^{FC} < P^{FC-\max} \times V_h^{FC} \tag{17}$$

2.3. CHP units model

In this paper, the electric and heat power generations of CHP units are assumed to be dependent on each other. For optimal power dispatch, two types of CHP units with different feasible operating regions (FORs) are considered [36]. The operating regions for each CHP are shown in Fig. 3. Relations (18)–(22) are used to present the features of the first type of CHP [6].

$$P_{i,h}^{CHP} - P_{i,A}^{CHP} - \frac{P_{i,A}^{CHP} - P_{i,B}^{CHP}}{H_{i,A}^{CHP} - H_{i,B}^{CHP}} \left(H_{i,h}^{CHP} - H_{i,A}^{CHP} \right) \leqslant 0 \tag{18}$$

$$P_{i,h}^{CHP} - P_{i,B}^{CHP} - \frac{P_{i,B}^{CHP} - P_{i,C}^{CHP}}{H_{i,B}^{CHP} - H_{i,C}^{CHP}} \left(H_{i,h}^{CHP} - H_{i,B}^{CHP} \right) \geqslant -\left(1 - V_{i,h}^{CHP}\right) \times M \tag{19}$$

$$P_{i,h}^{CHP} - P_{i,C}^{CHP} - \frac{P_{i,C}^{CHP} - P_{i,D}^{CHP}}{H_{i,C}^{CHP} - H_{i,D}^{CHP}} \left(H_{i,h}^{CHP} - H_{i,C}^{CHP} \right) \geqslant -\left(1 - V_{i,h}^{CHP}\right) \times M \tag{20}$$

$$0 \leqslant P_{i,h}^{CHP} \leqslant P_{i,A}^{CHP} \times V_{i,h}^{CHP} \tag{21}$$

$$0 \leqslant H_{i,h}^{CHP} \leqslant H_{i,B}^{CHP} \times V_{i,h}^{CHP} \tag{22}$$

In the abovementioned equations, M indicates a sufficient large number. Eq. (18) expresses the area under the curve AB. Eqs. (19) and (20) model the upper area of the curve BC, and the curve CD,

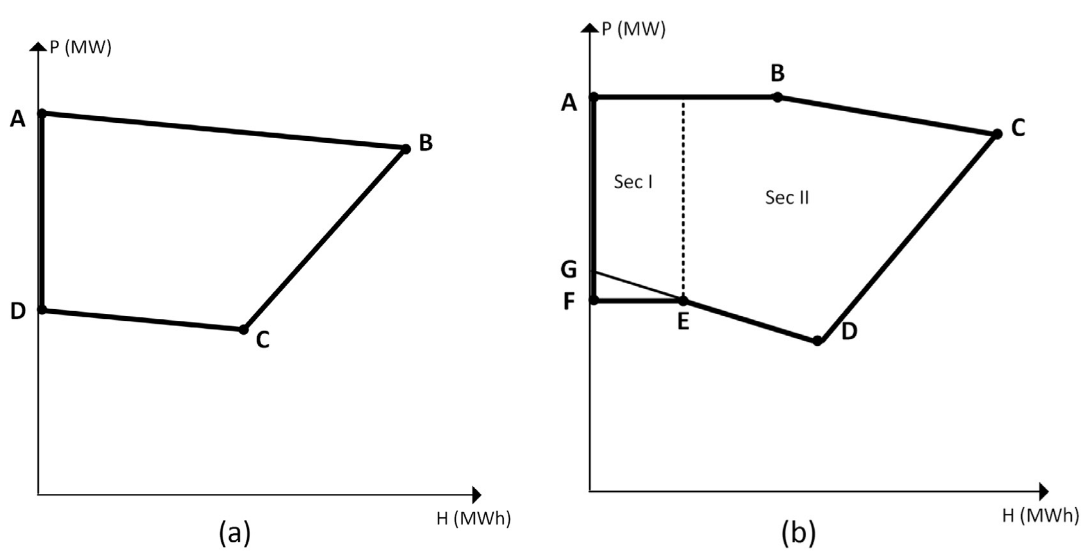

Fig. 3. Power-heat feasible region for CHP units. (a) Type 1. (b) Type 2.

respectively. According to Eqs. (19) and (20), when the binary variable $V_{i,h}^{CHP}$ is zero, the output power will be zero. Also, Eqs. (21) and (22) represent the power and heat generation limits, respectively.

According to Fig. 3, the FOR of second type is non-convex due to the bottom boundary of its performance area. In the second type of CHP, the gray region (FEG) would not be investigated because of implementing a traditional formulation such as the first FOR type formulation. Hence, this non-convex region is handled by implementing binary variables $X_{1,h}$ and $X_{2,h}$. Therefore, the non-convex FOR would be divided into two convex sub-regions I and II, as shown Fig. 3. 23 and 31 represent the power and heat generation limits for the second type of CHP [16].

$$P_{i,h}^{CHP} - P_{i,B}^{CHP} - \frac{P_{i,B}^{CHP} - P_{i,C}^{CHP}}{H_{i,B}^{CHP} - H_{i,C}^{CHP}}\left(H_{i,h}^{CHP} - H_{i,B}^{CHP}\right) \leqslant 0 \tag{23}$$

$$P_{i,h}^{CHP} - P_{i,C}^{CHP} - \frac{P_{i,C}^{CHP} - P_{i,D}^{CHP}}{H_{i,C}^{CHP} - H_{i,D}^{CHP}}\left(H_{i,h}^{CHP} - H_{i,C}^{CHP}\right) \geqslant 0 \tag{24}$$

$$P_{i,h}^{CHP} - P_{i,E}^{CHP} - \frac{P_{i,E}^{CHP} - P_{i,F}^{CHP}}{H_{i,E}^{CHP} - H_{i,F}^{CHP}}\left(H_{i,h}^{CHP} - H_{i,E}^{CHP}\right) \geqslant -(1 - X_{1,h}) \times M \tag{25}$$

$$P_{i,h}^{CHP} - P_{i,D}^{CHP} - \frac{P_{i,D}^{CHP} - P_{i,E}^{CHP}}{H_{i,D}^{CHP} - H_{i,E}^{CHP}}\left(H_{i,h}^{CHP} - H_{i,D}^{CHP}\right) \geqslant -(1 - X_{2,h}) \times M \tag{26}$$

$$0 \leqslant P_{i,h}^{CHP} \leqslant P_{i,A}^{CHP} \times V_{i,h}^{CHP} \tag{27}$$

$$0 \leqslant H_{i,h}^{CHP} \leqslant H_{i,C}^{CHP} \times V_{i,h}^{CHP} \tag{28}$$

$$X_{1,h} + X_{2,h} = V_{i,h}^{CHP} \tag{29}$$

$$H_{i,h}^{CHP} - H_{i,E}^{CHP} \leqslant (1 - X_{1,h}) \times M \tag{30}$$

$$H_{i,h}^{CHP} - H_{i,E}^{CHP} \geqslant -(1 - X_{2,h}) \times M \tag{31}$$

Eq. (23) expresses the area under the curve BC. The area over the curve CD is characterized using 24. Eqs. (25) and (26) depicted the upper areas of curves EF and DE, respectively. Eqs. (27) and (28) describe the maximum operation limits of the heat and power generation. In (29)–(31), $X_{1,h} = 1 (X_{2,h} = 1)$ means that the CHP unit operates in the first (second) convex section of FOR. According to 31, the operation region of the CHP unit would be either I or II when the unit is ON, and neither I nor II when the unit is OFF.

The total operation cost of a CHP unit is defined as [37]:

$$C\left(P_h^{CHP}, H_h^{CHP}\right) = a \times P_h^{CHP} + b \times P_h^{CHP} + c + d \times H_h^{CHP} + e \times H_h^{CHP} + f \times H_h^{CHP} \times P_h^{CHP}. \tag{32}$$

2.4. Power-only and heat-only model

The maximum operation limits of power- and heat-only units can be described as follows:

$$P_h^{PO-\min} \times V_h^{PO} \leqslant P_h^{PO} \leqslant P_h^{PO-\max} \times V_h^{PO} \tag{33}$$

$$H_h^{b-\min} \times V_h^{b} \leqslant H_h^{b} \leqslant H_h^{b-\max} \times V_h^{b} \tag{34}$$

The operation cost functions of a dispatchable power unit and boiler as heat-only units are assumed to be linear as follows:

$$C(P_h^{PO}) = \lambda_{po} \times P_h^{PO} \tag{35}$$

$$C(H_h^{b}) = \lambda_{b} \times H_h^{b} \tag{36}$$

The startup and shutdown status of the units is modeled by two binary variables $SU_{h,t}$ and $SD_{h,t}$ as follows:

$$SU_h^i = V_h^i \times (1 - V_{h-1}^i), \quad i \in FC, CHP, \mathrm{PO}, \mathrm{b} \tag{37}$$

$$SD_h^i = (1 - V_h^i) \times V_{h-1}^i, \quad i \in FC, CHP, \mathrm{PO}, \mathrm{b} \tag{38}$$

2.5. Electrical energy storage

Eqs. (39)–(42) express the ESS constraints [38]. Constraints (39) and (40) capture the limits on the charge and discharge of electrical power, as well as the level of energy stored in a battery unit. Here, the level of battery storage at the end of the scheduling horizon is equal to its initial energy level. Constraint (41) is imposed to ensure that the battery cannot be charged and discharged at the same time. The energy dynamic model of the battery is expressed in (42).

$$0 \leqslant P_{h,s}^{c} \leqslant b_{h,s}^{c} P_h^{c,\max}, \quad 0 \leqslant P_{h,s}^{disc} \leqslant b_{h,s}^{disc} P_h^{disc,\max} \tag{39}$$

$$E_k^{\min} \leqslant E_{h,s} \leqslant E_k^{\max} \tag{40}$$

$$b_{h,s}^{c} + b_{h,s}^{disc} \leqslant 1; \quad b_{h,s}^{c}, b_{h,s}^{disc} \in \{1, 0\} \tag{41}$$

$$E_{h+1,s} = E_{h,s} + \left(\eta^{C} \times P_{h,s}^{c} - \frac{P_{h,s}^{disc}}{\eta^{disc}}\right) \tag{42}$$

It should be noted that the battery does not charge and discharge simultaneously because of the unnecessary cost of charge and discharge efficiency deterioration.

2.6. Heat buffer tank

The heat buffer tank model is based on [22] and it is used for heat storage. The total generated heat H_h could be calculated as follows:

$$\overline{H}_h = \sum_{i=1}^{N_{CHP}} H_{i,h}^{CHP} + H_h^{b} + H_h^{FC} \tag{43}$$

The heat losses during shutdown and startup periods are shown by β_{gain} and β_{loss}, respectively. Therefore, the real heat H_h which is supported by the buffer is calculated as follows:

$$H_h = \overline{H}_h - \beta_{loss} \cdot SU_h^i + \beta_{gain} \cdot SD_h^i, \quad i \in FC, CHP, b \tag{44}$$

Moreover, the available heat capacity in each time interval in the heat buffer tank B_h is expressed as follows:

$$B_h = (1 - \eta) B_{h-1} + H_h - H_h^{load} \tag{45}$$

The maximum available capacity of heat storage is limited, as follows:

$$B_{\min} \leqslant B_h \leqslant B_{\max} \tag{46}$$

In this paper, the ramping up/down rates for the heat storage system are simulated as follows:

$$B_h - B_{h-1} \leqslant B_{\max}^{charge} \tag{47}$$

$$B_{h-1} - B_h \leqslant B_{\max}^{discharge} \tag{48}$$

2.7. Objective function

The FC-CHP-based MG scheduling problem is a multi-objective problem that maximizes the total profit and minimizes the emission function. Power sources supply the total power and heat demand of the MG. MG obtains revenue from selling the extra generated electricity in the power market when it is operated in the grid-connected mode which is described in the first term of OF_1. The cost of the MG includes the operational cost of units and startup and shutdown costs. The operational cost of CHP, FC, PO, the boiler, and the startup and shutdown costs are expressed in the objective function, mentioned in detail in the previous section. In the last term, the degradation cost of the battery storage device is formulated.

$$OF_1 = \sum_{t=1}^{N_h}\sum_{s=1}^{N_s}\pi_s \left\{ \begin{array}{l} \left(\lambda_{h,s} \times P_{h,s}^{G,sell} - \lambda_{h,s} \times P_{h,s}^{G,buy}\right) - \sum_{i=1}^{N_{CHP}} C\left(P_{i,h}^{CHP}, H_{i,h}^{CHP}\right) - C_{FC} \\ -C(P_h^{PO}) - C(H_h^b) - \sum_{j \in FC,CHP,PO,b} \left(C_{j,SU} \cdot SU_h^j + C_{j,SD} \cdot SD_h^j\right) \\ -C_k^{\deg}\left(\sum_{k=1}^{N_k} \frac{P_{k,h,s}^{disc}}{\eta_k^{disc}} + \eta_k^C \times P_{k,h,s}^c\right) \end{array} \right\} \tag{49}$$

The emission function for the grid and other generation units is calculated as follows [39]:

$$\begin{aligned} &OF_2 = Emission = \sum_{h=1}^{N_h}\left(E_h^{CHP} + E_h^{FC} + E_h^{PO} + E_h^G\right) \\ &E_h^{CHP} = \sum_{i=1}^{N_{CHP}} NOx_{i,h} + SO2_{i,h} + CO2_{i,h} = \left(k_1^{CHP} + k_2^{CHP} + k_3^{CHP}\right) \times P_{i,h}^{CHP} \\ &E_h^{FC} = NOx_h^{FC} + SO2_h^{FC} + CO2_h^{FC} = \left(k_1^{FC} + k_2^{FC} + k_3^{FC}\right) \times P_h^{FC} \\ &E_h^{PO} = NOx_h^{PO} + SO2_h^{PO} + CO2_h^{PO} = \left(k_1^{PO} + k_2^{PO} + k_3^{PO}\right) \times P_h^{PO} \\ &E_h^G = \sum_{s=1}^{N_s} NOx_{h,s}^G + SO2_{h,s}^G + CO2_{h,s}^G = \left(k_1^G + k_2^G + k_3^G\right) \times P_{h,s}^G \end{aligned} \tag{50}$$

The numerical values of these parameters are listed in Table 1.

2.7.1. Power balance

The power generation value in hth hour and in sth scenario should be equal to the load value, considering DR programs.

$$\pm P_{h,s}^G + \sum_{i=1}^{N_{CHP}} P_{i,h}^{CHP} + P_h^{FC} + P_h^{PO} + P_{h,s}^{disc} - P_{h,s}^c - P_{h,s}^{DR} = 0, \quad \forall \text{h, s.} \tag{51}$$

3. MG structure and assumptions

In this paper, three case studies have been taken into account:

Case A: CHP-FC-based MG scheduling in islanded mode;
Case B: CHP-FC-based MG scheduling in grid-connected mode;
Case C: Impact of TOU-DR program on MG scheduling.

In Cases B and C, the MG is able to exchange (sell or procure) power with the electric network, according to the pool market prices. The proposed stochastic programming model is applied to a typical MG. Maximum DR is assumed to be 30%.

Data of the fuel cell unit are listed in Table 2. Data of the energy storage device and heat buffer tank are presented in Tables 3 and 4, respectively. The startup and shutdown costs of units are presented in Table 5. Table 6 provides the cost function coefficients of CHP units. The FOR data of CHP units are also listed in this table.

Table 1
Emission factors related to NO_x, CO_2 and SO_2 (kg/MWh).

Emission type	Grid	CHP	FC	PO
NO_x	2.295	0.1995	0.5216	0.0136
CO_2	921.25	723.93	502.58	488.97
SO_2	3.583	0.0036	7.3627	0.0027

Table 2
Data of fuel cell unit.

Characteristics	Value	Characteristics	Value
$P^{FC-\max}$ (MW)	1.0	η^{st}	0.95
C_{ng} ($/MWh)	40	C_{pump} ($/MWh)	10
$P_{s,\max}^{FC-H_2}$ (MW/h)	0.5	$HT^{\max}$ (MWh)	2.0
$P_{dics,\max}^{FC-H_2}$ (MW/h)	0.5	OM ($/MWh)	10

Table 3
Data of energy storage device.

Characteristics	Value	Characteristics	Value
$P_{h,s}^c$	0.4	η^{disc}	0.9
$P_{h,s}^{disc}$	0.4	$\overline{ES}_{h,s}$	.8
η^C	0.9	$\underline{ES}_{h,s}$	0

Table 4
Data of the heat buffer tank.

Characteristics	Value	Characteristics	Value
β_{gain}	0.3	$B_{\max}^{charge}$	1
β_{loss}	0.6	$B_{\max}^{discharge}$	1
η	1%	$B^{\max}$	4

The base heat and electric demand of MG are shown in Fig. 4. As seen in this figure, the peak power demand is related to $t = 21$ h, in which the power demand is equal to 4.64 MW. Moreover, the minimum power demand occurs in $t = 4$ h, in which the magnitude of power demand is 1.0208 MW. The respective minimum and maximum heat demands of the studied MG occur in $t = 4$ h and $t = 21–22$ h, respectively. The heat demands for minimum and maximum peaks are respectively equal to 0.759 MW and 3.3 MW. In addition, electric power and heat price are shown in Fig. 5. Considering this figure, the maximum cost of electric power is in $t = 14$ h and the minimum price of power occurs in $t = 21$ h. Moreover, the minimum and maximum prices of heat occur in $t = 24$ h and $t = 11$ h, respectively. Finally, the mathematical modeling of the CHP-FC-based MG scheduling problem under stochastic process is solved using the SBB solver in the General Algebraic Modeling System (GAMS) environment.

4. The solution method

Consider a multi-objective mathematical program (MOMP) problem with k objective functions of $f_i(x)$.

$$\begin{aligned} &\max \quad (f_1(x), f_2(x), \ldots, f_k(x)) \\ &s.t. \\ &x \in S \end{aligned} \tag{52}$$

In which the vector of decision variables and the feasible region are demonstrated by x and S, respectively.

The ε-constraint method is an approach in which one of the objective functions of the MOMP problem is optimized by taking into account the other objective functions as constraints of the problem. The other objective functions are incorporated to the feasible solution space of S, which can be stated as:

$$\begin{aligned} &\max f_1(x) \\ &s.t. \\ &f_2(x) \geqslant \varepsilon_2, \\ &f_3(x) \geqslant \varepsilon_3, \\ &\ldots \\ &f_k(x) \geqslant \varepsilon_k, \\ &x \in S \end{aligned} \tag{53}$$

Table 5
Cost data of startup and shutdown of generation units.

Unit/characteristics	CSU	CSD	Unit/characteristics	CSU	CSD
CHP unit 1	20	20	Power only unit	12	12
CHP unit 2	20	20	Heat only unit	9	9

Table 6
Data of cogeneration units.

In cost function	CHP unit 1	CHP unit 2	In feasible region	CHP unit 1	CHP unit 2
a	0.0435	0.0345	A (p, h)	(2.47, 0)	(1.258, 0)
b	56	44.5	B (p, h)	(2.15, 1.8)	(1.258, 0.324)
c	12.5	26.5	C (p, h)	(0.81, 1.048)	(1.102, 1.356)
d	0.027	0.03	D (p, h)	(0.988, 0)	(0.4, 0.75)
e	0.6	4.2	E (p, h)	–	(0.44, 0.159)
f	0.011	0.031	F (p, h)	–	(0.44, 0)

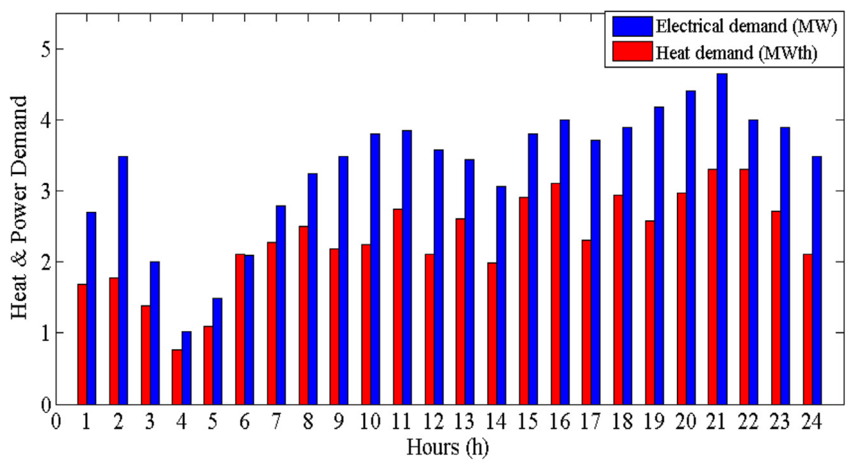

Fig. 4. Electric power and heat demand.

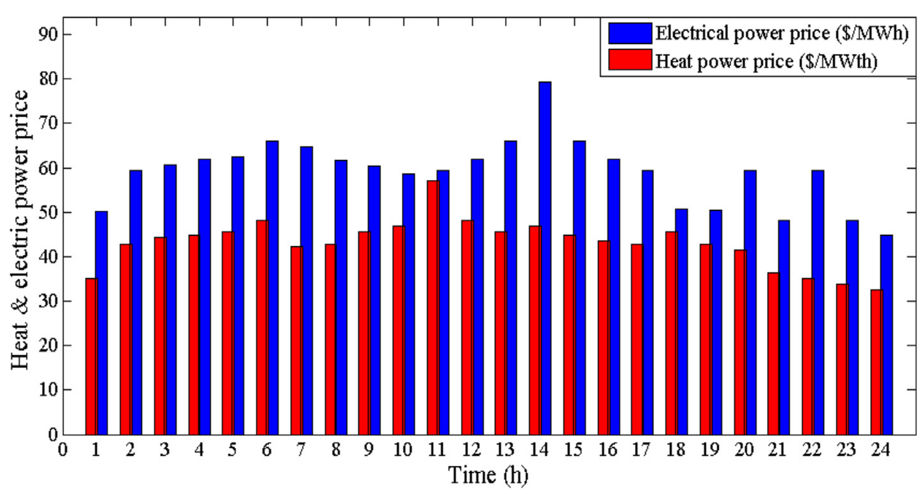

Fig. 5. Electric power and heat price.

To provide the optimal solution, the right-hand sides of the incorporated constraints $(\varepsilon_2, \varepsilon_3, \ldots, \varepsilon_k)$ are altered parametrically. To define grid points for the amount of $(\varepsilon_2, \varepsilon_3, \ldots, \varepsilon_k)$, the range of at least $k - 1$ objective functions is required.

4.1. Fuzzy decision maker

The fuzzy decision maker is employed in this paper in order to choose the best solution from a provided Pareto optimal set which is attained by solving the optimization problem. The fuzzy decision maker assigns a fuzzy membership function to each solution in the Pareto front, which is in the interval [0, 1]. To obtain linear fuzzy membership functions for the i-th objective function of the f_k, the following equation can be utilized [40]:

$$\hat{f}_k = \left\{ \begin{array}{ll} 1 & f_k \leqslant f_k^L \\ \frac{f_k^{\max} - f_k}{f_k^{\max} - f_k^{\min}} & f_k^L \leqslant f_k \leqslant f_k^U \\ 0 & f_k \geqslant f_k^U \end{array} \right\} \tag{54}$$

Table 7
Pareto optimal solutions for short-term scheduling of micro-grid without DRP (Case-A).

#	Power only unit cost ($/day)	FC unit cost ($/day)	CHP unit cost ($/day)	Total cost of MG ($/day)	Emission (ton/day)	Φ_1 (p.u.)	Φ_2 (p.u.)
1	818.75	582.93	2632.67	4231.196	64472.89	1.183	0.010
2	783.36	627.82	2632.27	4240.289	64184.42	1.171	0.050
3	747.96	672.71	2631.88	4249.387	63895.94	1.160	0.100
4	712.56	717.59	2631.49	4258.488	63607.47	1.148	0.150
5	695.13	752.61	2624.00	4268.572	63318.99	1.136	0.200
6	693.58	783.01	2609.98	4283.424	63030.51	1.117	0.250
7	693.58	813.33	2595.33	4299.079	62742.04	1.097	0.300
8	693.58	843.64	2580.69	4314.747	62453.56	1.078	0.350
9	693.58	873.95	2566.18	4330.55	62165.09	1.058	0.400
10	696.71	902.40	2550.5	4346.44	61876.61	1.038	0.450
11	697.13	932.72	2537.34	4364.025	61588.13	1.016	0.500
12	770.73	932.72	2493.01	4393.302	61299.66	0.979	0.550
13	883.86	939.00	2434.47	4512.91	61011.18	0.829	0.600
14	917.95	932.72	2404.40	4451.911	60722.71	0.906	0.650
15	991.56	932.72	2360.37	4481.488	60434.23	0.868	0.700
16	**1060.52**	**937.49**	**2321.56**	**4516.408**	**60145.75**	**0.825**	**0.750**
17	1144.09	927.26	2271.38	4579.575	59857.28	0.745	0.800
18	1271.03	918.26	2259.42	4690.39	59568.8	0.606	0.850
19	1314.00	932.31	2225.35	4770.276	59280.33	0.506	0.900
20	1361.61	936.83	2198.77	4730.235	58991.85	0.556	0.950

The min-max method is implemented to obtain the best compromise solution. The basic process of the min-max method is obtaining the minimum value of f_1 and f_2, and choosing the solution with the maximum value of min $(\hat{f}_1, \hat{f}_2)$ as the best compromise solution.

5. Simulation results

Case Study A: *CHP-FC-based MG scheduling in islanded mode*: In this case, the islanded mode is taken into account for MG. Table 7 provides the Pareto optimal solutions for short-term scheduling of MG without consideration of DRP for Case A. Twenty iterations are taken into account to generate Pareto optimal solutions. The maximum weakest membership function of 0.750 is related to Solution #16. Considering the min-max fuzzy satisfying method, Solution #16 is opted as the best compromise solution. According to Table 7, the costs of energy supply for the optimal solution utilizing the power-only unit, FC unit, and CHP unit, are $1060.52, $937.49, and $2321.56, respectively. Hence, the cost of MG energy production is equal to $4516.408. Moreover, the emission is obtained as 60145.75 ton/day. The minimum value of operation cost of MG is obtained as $4231.196, which is related to Solution #1 where the aim is to minimize the total cost of MG. Also, the minimum amount of emission provided is equal to 58991.85 ton/day, which is obtained in Solution #20 where the minimization of emission is aimed. Fig. 6 shows the produced power of Case A for the time horizon of 24 h. As seen in this figure, fuel cell, CHP1, and CHP2 have participated in power production in the scheduling time horizon of 24 h. Additionally, CHP1 and CHP2 have participated in power production more than other generation units. The fuel cell has produced power with half of the power supply capacity. Moreover, the power-only unit has not taken part in power production between 1:00 and 6:00 due to its high production cost in comparison with other generation units.

The supplied heat of Case A in the studied time horizon is illustrated in Fig. 7. According to this figure, the heat generation of CHP1 is more than those of other production units. CHP2 has less heat generation than CHP1, since its heat cost is higher than that of CHP1. In addition, considering the high cost function of the boiler in comparison with other generation units, the boiler will not take part in heat generation. The fuel cell has produced heat in its capacity limits. As it is obvious in Figs. 6 and 7, considering the time interval at which the fuel cell has not participated in power and heat generation, the remained capacity of the fuel cell is stored as hydrogen in the hydrogen tank at this time interval.

Case Study B: *CHP-FC-based MG scheduling in grid-connected mode*: In this mode, the capability of energy exchange with the grid

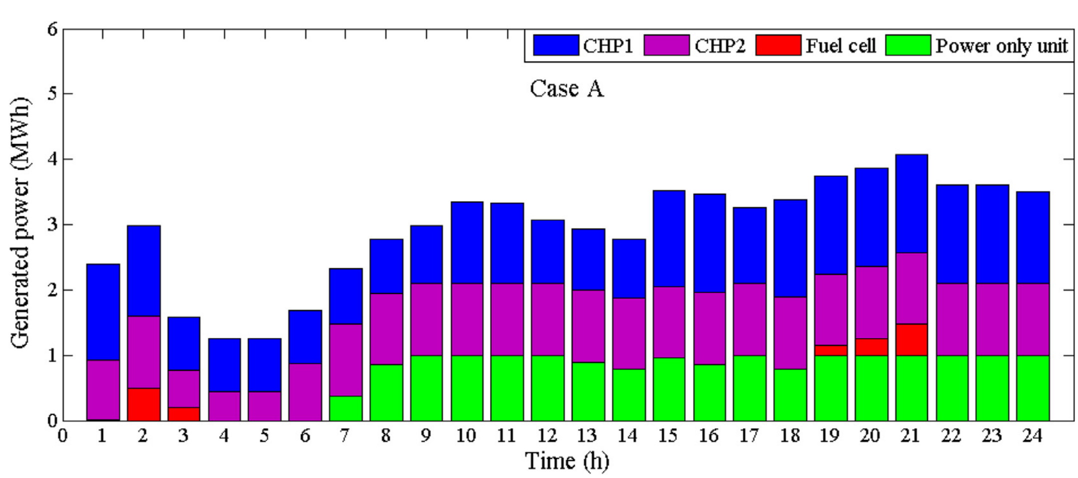

Fig. 6. Generated power of the case A.

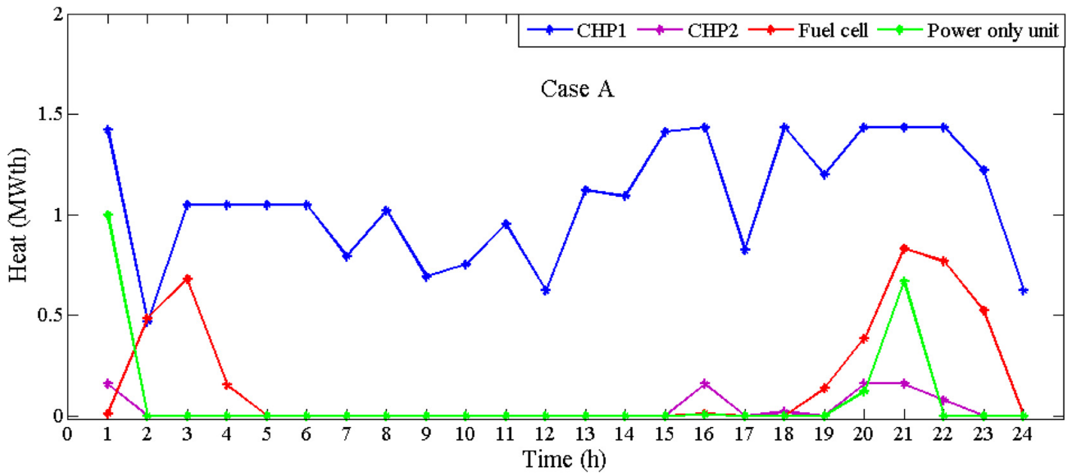

Fig. 7. Generated heat of the case A.

is considered. The Pareto optimal solutions for short-term scheduling of MG in this mode are shown in Table 8. The maximum weakest membership function which is equal to 0.85 is related to Solution #18. Taking into account the min-max fuzzy satisfying method, Solution #18 is selected as the best compromise solution. The respective costs of energy generation of power-only unit, FC unit, and CHP unit of Solution #18 as the best compromise solution are $1306.355, $902.212, and $2638.325, respectively. Accordingly, the cost of MG energy supply is equal to $3769.579. Moreover, the emission of the best compromise solution is obtained as 53590.722 ton/day. In Solution #1, which is focused on the minimization of the total cost of MG, the minimum value of MG is obtained as S3711.545, whereas Solution #20 aims to obtain the minimum emission which is equal to 53080.028 ton/day. Figs. 8 and 9 illustrate the generated power and heat of Case B, respectively. As shown in Fig. 8, CHP1 and CHP2 have participated in power generation during the scheduled time horizon. Considering the interconnection of MG and network, the MG has sold a part of power demand to the network until 17:00, and has supplied a part of power demand from the network between 18:00 and 24:00. Taking into consideration the higher power generation cost of the power-only unit with respect to other units, it has less participation in power production than other units. Moreover, CHP1 and CHP2 have contributed in power production continuously. According to Fig. 9, the heat production of CHP1 unit is more than those of other production units, because its cost function is less than those of other units. Moreover, the cost function of the boiler is high in comparison with other generation units, and the boiler will not take part in heat generation.

Case Study C: *The impact of TOU-DR program on MG scheduling:* This case is analyzed for the determination of DRP's impact on the solution of MG scheduling. The Pareto optimal solutions for short-term scheduling of MG with the consideration of DRP are provided in Table 9. The maximum weakest membership function considering the prepared solutions in this table is equal to 0.899, which is related to Solution #19. According to the min-max fuzzy satisfying method, Solution#19 is the best compromise solution. As shown in Table 9, the costs of energy generation of the power-only unit, FC unit, and CHP unit are $1351.36, $928.21, and $2635.98, respectively. Thus, the cost of MG energy supply is $3652.031. The emission is this mode is obtained as 53150.16 ton/day. The MG cost minimization is aimed in Solution #1 in which the minimum value of $3601.079 is obtained for the cost of MG. Emission is minimized in Solution #20 where the minimum amount of emission is obtained as 60213.29 ton/day.

Fig. 10 illustrates the supplied power of Case C in the time horizon of 24 h. As seen in this figure, CHP1, CHP2, and fuel cell have participated in power supply during the whole scheduled time. It

Table 8
Pareto optimal solutions for short-term scheduling of micro-grid without DRP (Case-B).

#	Power only unit cost ($/day)	FC unit cost ($/day)	CHP unit cost ($/day)	Total cost of MG ($/day)	Emission (ton/day)	Φ_1 (p.u.)	Φ_2 (p.u.)
1	1326.451	225.548	2640.056	3711.545	62514.813	1.01	0.026
2	1326.451	238.782	2639.939	3711.734	62272.520	1	0.05
3	1326.451	286.765	2641.016	3711.661	61761.826	1	0.1
4	1326.451	327.809	2640.848	3712.007	61251.132	0.99	0.15
5	1326.451	369.720	2641.216	3712.841	60740.438	0.99	0.2
6	1326.451	404.693	2641.278	3713.916	60229.744	0.99	0.25
7	1327.534	443.400	2641.085	3715.068	59719.050	0.99	0.3
8	1326.451	479.640	2641.071	3716.312	59208.356	0.98	0.35
9	1342.696	508.201	2641.260	3717.620	58697.662	0.98	0.4
10	1360.239	535.815	2641.188	3719.163	58186.968	0.98	0.45
11	1360.239	576.858	2640.822	3720.968	57676.274	0.97	0.5
12	1360.239	618.481	2641.079	3722.859	57165.580	0.97	0.55
13	1360.239	660.392	2640.831	3725.150	56654.886	0.96	0.6
14	1318.313	718.859	2640.581	3729.073	56144.192	0.95	0.65
15	1354.985	739.168	2639.507	3735.327	55633.498	0.94	0.7
16	1354.985	781.080	2638.770	3743.280	55122.804	0.92	0.75
17	1354.985	823.463	2638.416	3754.260	54612.110	0.90	0.8
18	**1306.355**	**902.212**	**2638.325**	**3769.579**	**54101.416**	**0.86**	**0.85**
19	1257.224	982.078	2633.506	3790.603	53590.722	0.82	0.9
20	1367.811	1005.023	2603.701	3827.754	53080.028	0.73	0.95

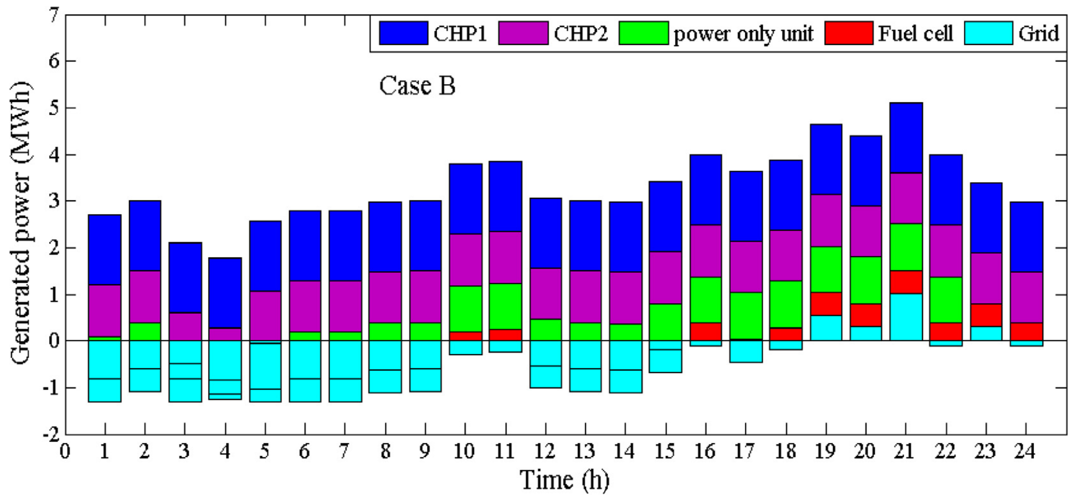

Fig. 8. Generated power of the case B.

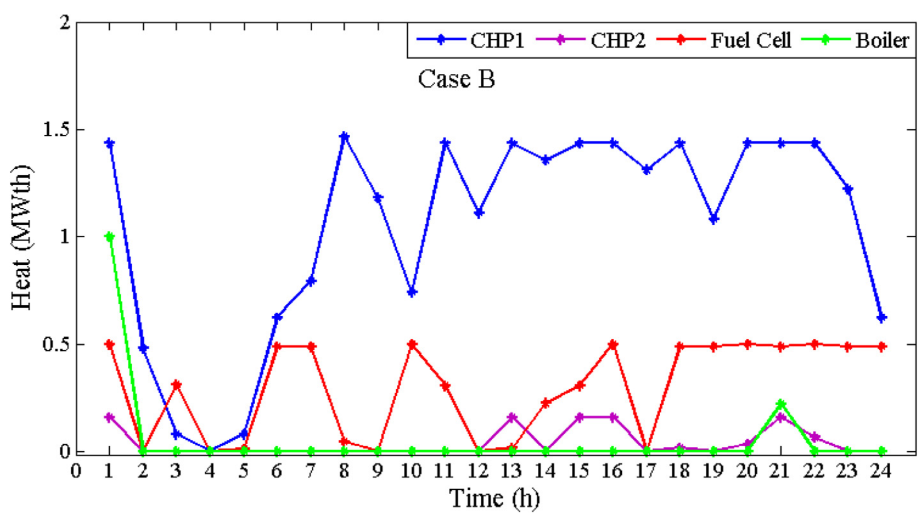

Fig. 9. Generated heat of the case B.

Table 9
Pareto optimal solutions for short-term scheduling of micro-grid considering DRP (Case-C).

#	Power only unit cost ($/day)	FC unit cost ($/day)	CHP unit cost ($/day)	Total cost of MG ($/day)	Emission (ton/day)	Φ_1 (p.u.)	Φ_2 (p.u.)
1	1436.78	297.63	2640.16	3601.079	60213.29	1.040	0.03
2	1436.78	309.23	2640.06	3601.088	60071.99	1.040	0.05
3	1436.78	342.64	2639.77	3601.457	59664.82	1.039	0.1
4	1436.78	376.06	2639.14	3602.322	59257.66	1.036	0.15
5	1436.78	407.53	2638.95	3603.445	58850.49	1.033	0.2
6	1436.78	440.94	2638.65	3604.811	58443.32	1.029	0.25
7	1436.78	474.36	2638.35	3606.243	58036.16	1.025	0.3
8	1436.78	507.77	2638.06	3607.677	57628.99	1.021	0.35
9	1436.78	541.19	2637.76	3609.113	57221.82	1.017	0.4
10	1436.78	574.60	2637.47	3610.553	56814.66	1.014	0.45
11	1436.78	608.02	2637.18	3612.079	56407.49	1.009	0.5
12	1436.78	641.43	2636.98	3613.857	56000.32	1.004	0.55
13	1436.78	674.85	2637.23	3615.854	55593.16	0.999	0.6
14	1436.78	708.26	2637.52	3617.935	55185.99	0.993	0.65
15	1410.77	751.95	2637.39	3620.725	54778.82	0.985	0.7
16	1399.76	789.71	2636.13	3625.064	54371.66	0.973	0.75
17	1399.76	826.92	2636.03	3631.378	53964.49	0.956	0.8
18	1399.76	864.24	2636.00	3638.824	53557.32	0.935	0.85
19	**1351.36**	**928.21**	**2635.98**	**3652.031**	**53150.16**	**0.899**	**0.9**
20	1371.01	969.56	2612.20	3677.299	52742.99	0.829	0.95

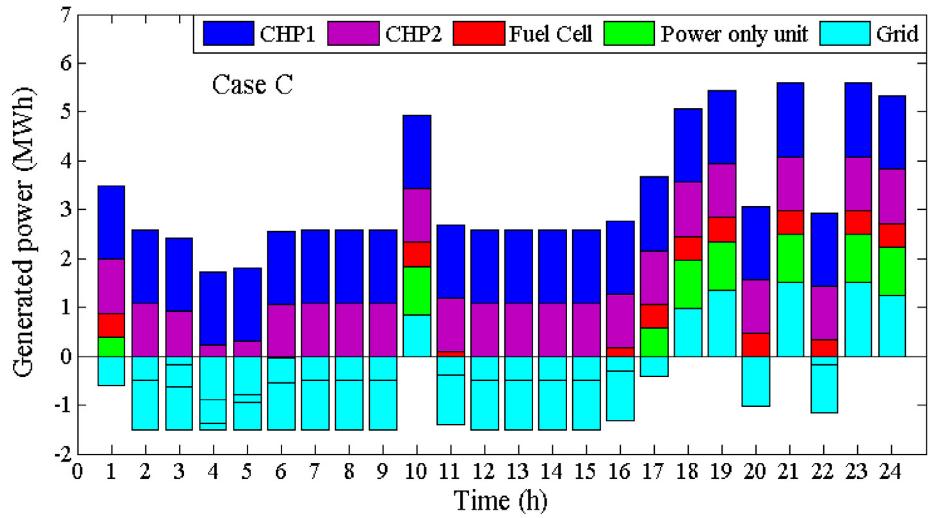

Fig. 10. Generated power of the case C.

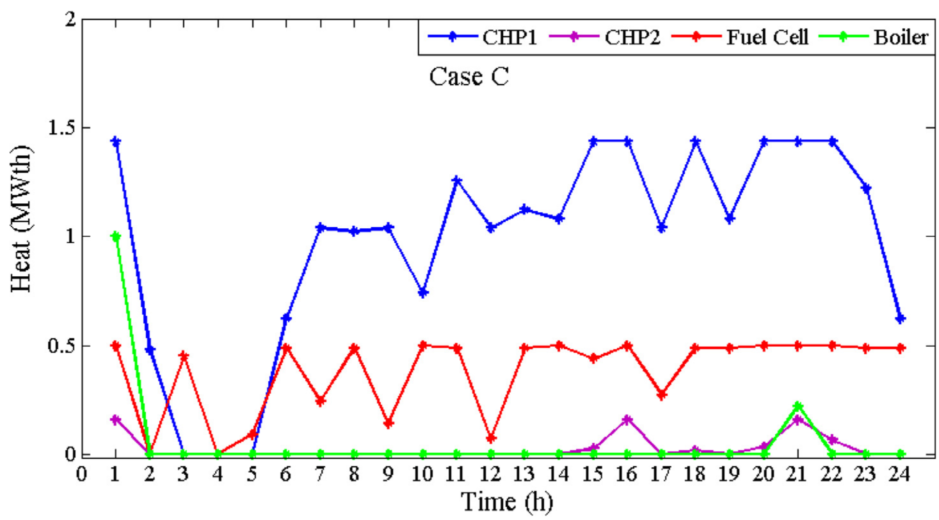

Fig. 11. Generated heat of the case C.

is obvious that the power-only unit has less contribution to the generation of power, since it has a higher cost level compared to other generation units. According to this figure, MG and the network can transfer power to each other. MG has sold power to the network until 9:00 and between 11:00 and 17:00. Also, the power is sold to the network at 20:00 and 22:00. The heat generated in this time horizon is shown in Fig. 11. The participation of CHP1 and fuel cell in the heat generation of MG is obvious, in which CHP1 has produced more heat than CHP2 due to its low cost function. Additionally, CHP2 and the boiler have less contribution to the heat generation of MG, since their cost functions are higher than those of other generation units. It should be noted that the heat generation of the fuel cell is low between 11:00 to 13:00; it produced hydrogen in this time interval, and the generated hydrogen has been stored in the hydrogen tank. The demand levels with consideration of DRP (in Scenarios 3 and 5) are demonstrated in Fig. 12.

The hydrogen production of the three studied modes is depicted in Fig. 13. As mentioned before, considering the decreased production level of the fuel cell between 2:00 and 4:00 in the studied cases, the fuel cell has produced hydrogen and the generated hydrogen has been stored in the hydrogen tank. In Case 3, after the generated hydrogen has been stored, it has been utilized in order to produce energy at 4:00. In Case C, the generated hydrogen is stored in the hydrogen tank until 23:00 and then is utilized in order to supply electricity.

6. Conclusion

In this paper, the short-term scheduling of a fuel cell-combined heat and power-based MG is taken into account. The components of the MG are an FC unit, CHP generation units, power-only unit, boiler, battery storage system, and heat buffer tank. The characteristics of heat and power's dual dependency have been modeled for the two types of CHP units by employing a mixed integer linear formulation. The economic model of the operational cost of the FC has been developed which includes power trade with the grid, thermal recovery, and hydrogen production/storage. The power demands of the customer have been supplied considering the time-of-use-based demand response (DR) program. The proposed

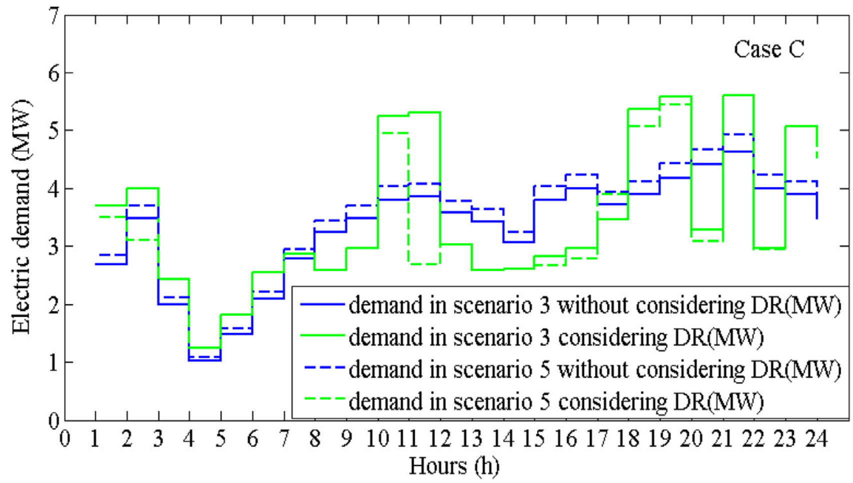

Fig. 12. Demand levels with considering DRP (in scenario 3 and 5).

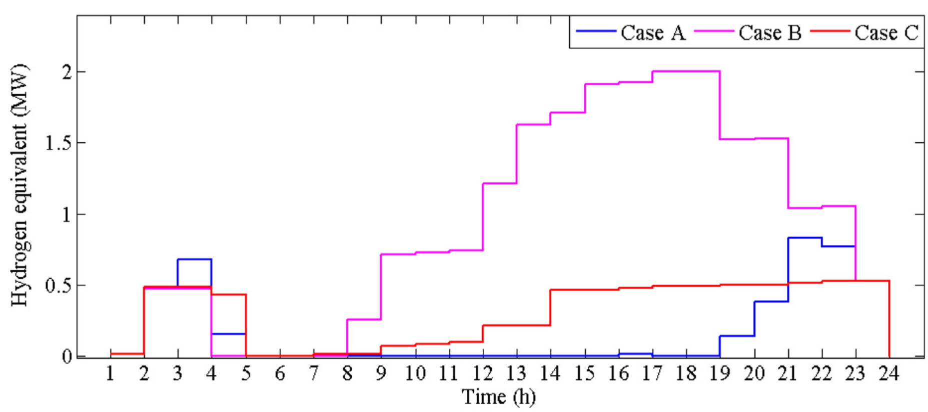

Fig. 13. Hydrogen production in three operation modes.

cost and emission functions are optimized simultaneously in a multi-objective optimization framework. The ε-constraint method is used to solve the multi-objective optimization problem. In this study, three cases are analyzed to verify the performance of the proposed approach, including islanded mode, grid-connected mode, and impact of TOU-DR program on the MG scheduling. In Case A, MG is considered in the islanded mode and the cost of MG energy production is $4516.408 for the best compromise solution. Moreover, the emission of this solution is obtained as 60145.75 ton/day. In Case B, MG is in the grid-connected mode and the energy costs of MG and emission are decreased to $3790.603 and 53590.722 ton/day, respectively, for the best compromise solution. By implementing the DR program in Case C, the respective cost function and emission are $3652.031 and 53150.16 ton/day, respectively.

References

[1] Y. Zhang, N. Gatsis, G.B. Giannakis, Robust energy management for microgrids with high-penetration renewables, IEEE Trans. Sustain. Energy 4 (2013) 944–953.
[2] Q. Jiang, M. Xue, G. Geng, Energy management of microgrid in grid-connected and stand-alone modes, IEEE Trans. Power Syst. 28 (2013) 3380–3389.
[3] A.K. Basu, A. Bhattacharya, S. Chowdhury, S. Chowdhury, Planned scheduling for economic power sharing in a CHP-based micro-grid, IEEE Trans. Power Syst. 27 (2012) 30–38.
[4] A. Haghrah, M. Nazari-Heris, B. Mohammadi-ivatloo, Solving combined heat and power economic dispatch problem using real coded genetic algorithm with improved Mühlenbein mutation, Appl. Therm. Eng. 99 (2016) 465–475.
[5] W.C. Long, R. Luck, P.J. Mago, Uncertainty based operating strategy selection in combined heat and power systems, Appl. Therm. Eng. 98 (2016) 1013–1024.
[6] B. Mohammadi-Ivatloo, M. Moradi-Dalvand, A. Rabiee, Combined heat and power economic dispatch problem solution using particle swarm optimization with time varying acceleration coefficients, Electric Power Syst. Res. 95 (2013) 9–18.
[7] M. Alipour, K. Zare, B. Mohammadi-Ivatloo, Short-term scheduling of combined heat and power generation units in the presence of demand response programs, Energy 71 (2014) 289–301.
[8] H. Damirchi, G. Najafi, S. Alizadehnia, R. Mamat, C.S.N. Azwadi, W. Azmi, M. Noor, Micro combined heat and power to provide heat and electrical power using biomass and Gamma-type Stirling engine, Appl. Therm. Eng. 103 (2016) 1460–1469.
[9] M. Motevasel, A.R. Seifi, Expert energy management of a micro-grid considering wind energy uncertainty, Energy Convers. Manage. 83 (2014) 58–72.
[10] M.H. Ahmadi, S.S.G. Aghaj, A. Nazeri, Prediction of power in solar stirling heat engine by using neural network based on hybrid genetic algorithm and particle swarm optimization, Neural Comput. Appl. 22 (2013) 1141–1150.
[11] M.H. Ahmadi, M.A. Ahmadi, S.A. Sadatsakkak, M. Feidt, Connectionist intelligent model estimates output power and torque of stirling engine, Renew. Sustain. Energy Rev. 50 (2015) 871–883.
[12] S.M. Pourkiaei, M.H. Ahmadi, S.M. Hasheminejad, Modeling and experimental verification of a 25W fabricated PEM fuel cell by parametric and GMDH-type neural network, Mech. Ind. 17 (2016) 105.
[13] J.-H. Teng, Y.-H. Liu, C.-Y. Chen, C.-F. Chen, Value-based distributed generator placements for service quality improvements, Int. J. Electr. Power Energy Syst. 29 (2007) 268–274.
[14] S. Bae, A. Kwasinski, Dynamic modeling and operation strategy for a microgrid with wind and photovoltaic resources, IEEE Trans. Smart Grid 3 (2012) 1867–1876.
[15] M. Alipour, B. Mohammadi-Ivatloo, K. Zare, Stochastic scheduling of renewable and CHP-based microgrids, IEEE Trans. Industr. Inf. 11 (2015) 1049–1058.
[16] H.K. Nunna, S. Doolla, Energy management in microgrids using demand response and distributed storage—a multiagent approach, IEEE Trans. Power Delivery 28 (2013) 939–947.

[17] H.K. Nunna, S. Doolla, Multiagent-based distributed-energy-resource management for intelligent microgrids, IEEE Trans. Industr. Electron. 60 (2013) 1678–1687.

[18] J. Aghaei, M.-I. Alizadeh, Multi-objective self-scheduling of CHP (Combined heat and power)-based microgrids considering demand response programs and ESSs (energy storage systems), Energy 55 (2013) 1044–1054.

[19] K.H. Nunna, S. Doolla, Responsive end-user-based demand side management in multimicrogrid environment, IEEE Trans. Industr. Inf. 10 (2014) 1262–1272.

[20] H.K. Nunna, A.M. Saklani, A. Sesetti, S. Battula, S. Doolla, D. Srinivasan, Multi-agent based Demand Response management system for combined operation of smart microgrids, Sustain. Energy, Grids Networks 6 (2016) 25–34.

[21] S. Mohammadi, S. Soleymani, B. Mozafari, Scenario-based stochastic operation management of microgrid including wind, photovoltaic, micro-turbine, fuel cell and energy storage devices, Int. J. Electr. Power Energy Syst. 54 (2014) 525–535.

[22] M. Shahverdi, S. Moghaddas-Tafreshi, Operation optimization of fuel cell power plant with new method in thermal recovery using particle swarm algorithm, in: Electric Utility Deregulation and Restructuring and Power Technologies, 2008. DRPT 2008. Third International Conference on, IEEE, 2008, pp. 2542–2547.

[23] M. El-Sharkh, A. Rahman, M. Alam, Evolutionary programming-based methodology for economical output power from PEM fuel cell for micro-grid application, J. Power Sources 139 (2005) 165–169.

[24] T. Niknam, A.K. Fard, A. Baziar, Multi-objective stochastic distribution feeder reconfiguration problem considering hydrogen and thermal energy production by fuel cell power plants, Energy 42 (2012) 563–573.

[25] G. Cau, D. Cocco, M. Petrollese, S.K. Kær, C. Milan, Energy management strategy based on short-term generation scheduling for a renewable microgrid using a hydrogen storage system, Energy Convers. Manage. 87 (2014) 820–831.

[26] D. Shapiro, J. Duffy, M. Kimble, M. Pien, Solar-powered regenerative PEM electrolyzer/fuel cell system, Sol. Energy 79 (2005) 544–550.

[27] V. Rangel-Hernandez, C. Damian-Ascencio, D. Juarez-Robles, A. Gallegos-Muñoz, A. Zaleta-Aguilar, H. Plascencia-Mora, Entropy generation analysis of a proton exchange membrane fuel cell (PEMFC) with a fermat spiral as a flow distributor, Energy 36 (2011) 4864–4870.

[28] M.H. Ahmadi, M.A. Ahmadi, S.A. Sadatsakkak, Thermodynamic analysis and performance optimization of irreversible Carnot refrigerator by using multi-objective evolutionary algorithms (MOEAs), Renew. Sustain. Energy Rev. 51 (2015) 1055–1070.

[29] M.H. Ahmadi, M.A. Ahmadi, A. Mellit, F. Pourfayaz, M. Feidt, Thermodynamic analysis and multi objective optimization of performance of solar dish Stirling engine by the centrality of entransy and entropy generation, Int. J. Electr. Power Energy Syst. 78 (2016) 88–95.

[30] V. Punnathanam, P. Kotecha, Effective multi-objective optimization of Stirling engine systems, Appl. Therm. Eng. 108 (2016) 261–276.

[31] S.A. Sadatsakkak, M.H. Ahmadi, M.A. Ahmadi, Thermodynamic and thermo-economic analysis and optimization of an irreversible regenerative closed Brayton cycle, Energy Convers. Manage. 94 (2015) 124–129.

[32] S.A. Sadatsakkak, M.H. Ahmadi, R. Bayat, S.M. Pourkiaei, M. Feidt, Optimization density power and thermal efficiency of an endoreversible Braysson cycle by using non-dominated sorting genetic algorithm, Energy Convers. Manage. 93 (2015) 31–39.

[33] M.H. Ahmadi, M.-A. Ahmadi, M. Feidt, Thermodynamic analysis and evolutionary algorithm based on multi-objective optimization of performance for irreversible four-temperature-level refrigeration, Mech. Ind. 16 (2015) 207.

[34] S. Abapour, K. Zare, B. Mohammadi-Ivatloo, Dynamic planning of distributed generation units in active distribution network, IET Gener. Transm. Distrib. 9 (2015) 1455–1463.

[35] M. El-Sharkh, M. Tanrioven, A. Rahman, M. Alam, Economics of hydrogen production and utilization strategies for the optimal operation of a grid-parallel PEM fuel cell power plant, Int. J. Hydrogen Energy 35 (2010) 8804–8814.

[36] M. Alipour, K. Zare, B. Mohammadi-Ivatloo, Optimal risk-constrained participation of industrial cogeneration systems in the day-ahead energy markets, Renew. Sustain. Energy Rev. 60 (2016) 421–432.

[37] G. Piperagkas, A. Anastasiadis, N. Hatziargyriou, Stochastic PSO-based heat and power dispatch under environmental constraints incorporating CHP and wind power units, Electric Power Syst. Res. 81 (2011) 209–218.

[38] D.T. Nguyen, L.B. Le, Optimal bidding strategy for microgrids considering renewable energy and building thermal dynamics, IEEE Trans. Smart Grid 5 (2014) 1608–1620.

[39] T. Niknam, A. Kavousifard, S. Tabatabaei, J. Aghaei, Optimal operation management of fuel cell/wind/photovoltaic power sources connected to distribution networks, J. Power Sources 196 (2011) 8881–8896.

[40] S. Mohseni-Bonab, A. Rabiee, S. Jalilzadeh, B. Mohammadi-Ivatloo, S. Nojavan, Probabilistic multi objective optimal reactive power dispatch considering load uncertainties using Monte Carlo simulations, J. Oper. Automat. Power Eng. 3 (2015) 83–93.